ELECTRONIC SUPPORTING INFORMATION

Green Synthesis of Imine-based Covalent Organic Frameworks in Water

Jesús Á. Martín-Illán, David Rodríguez-San-Miguel, Carlos Franco, Inhar Imaz, Daniel Maspoch, Josep Puigmartí-Luis*, and Félix Zamora*

Table of Contents

Section S1. Experimental Section

Materials

1,3,5-tris(4-aminophenyl)benzene (TAPB) was synthesized as previously reported[1] 1,3,5-benzenetricarbaldehyde (BTCA) and hydrazine monohydrate (HZ) were purchased from Sigma Aldrich Co. 2,4,6-tris(4-aminophenyl)-1,3,5-triazine (TZ) was purchased from Fluorochem Co. Ethanol and acetic acid were purchased from Scharlab. Water was purified with a Milli-Q® system.

Methods

Elemental Analysis were obtained using a LECO CHNS-932 elemental analyser.

Powder X-ray diffraction (PXRD) patterns were collected with a Bruker D8 Advance X-ray diffractometer (Cu-Kα radiation; λ = 1.5418 Å) equipped with a Lynxeye detector. Samples were mounted on a glass flat sample plate. Patterns were collected in the $3.5° < 2\theta < 35°$ range with a step size of 0.03° and exposure time of 1.3 s/step.

Fourier transform infrared (FT-IR) spectra were recorded in a Perkin Elmer Spectrum 100 with a PIKE Technologies MIRacle Single Reflection Horizontal ATR (attenuated total reflection) accessory with a spectral range of 4000-650 cm^{-1}, signals are given in wavenumbers (cm^{-1}).

Solid-State ^{13}C CP-MAS Nuclear Magnetic Resonance Spectroscopy were recorded at room temperature on a Bruker AV 400 WB spectrometer using a triple channel, 4 mm probe with zirconia rotors and a Kel-F cap. Cross-polarization with Magic Angle Spinning (CP-MAS) was used to acquire ^{13}C data at 100.61 MHz. The spectral width of the pulse sequence was 35 kHz and the ^{1}H excitation pulse was 3 µs. The CP contact time was 3.5 ms. High power two-pulse phase modulation (TPPM) ^{1}H decoupling was applied during data acquisition using a decoupling frequency of 80 kHz. Recycle delays were 4 s and the sample spinning rate was 10 kHz.

Thermogravimetric analyses (TGA) were run on a Thermobalance TGA Q-500 thermal gravimetric analyser with samples held in an aluminium pan under nitrogen atmosphere. The samples were heated at 10 K min^{-1} within a temperature range of 25-1000^{o}C.

N_2 adsorption and desorption isotherms were done at 77 K using an Autosorb-IQ-AG analyser (Quantachrome Instruments). Prior to measurement, samples were heated at 323 K overnight and outgassed to 10^{-6} Torr. The accessible geometrical surface areas were calculated by Poreblazer software.[2] Additionally, the Connolly surface of the crystal models were determined with a 1.4 Å van der Waals scale factor and 1.84 Å. Connolly radius using Material Studio.[3]

Scanning Electron Microscopy (SEM) studies were performed on a Philips XL 30 S-FEG microscope operating at an accelerating voltage of 10 kV. Samples were previously coated with chromium in a sputter Quorum Q150T-S. The samples were prepared simply by putting a drop of COFs dispersed in water on a clean piece of silicon oxide.

Critical point drying was performed in a SPI-DRY Critical Point Dryer-Jumbo First according to the following method. First, the solid inside a filter paper bag was loaded into the chamber of the critical point dryer. Then, the chamber was filled with liquid CO_2 at 283 K and 50 bar. After 30 minutes, the chamber was flushed with fresh liquid CO_2. This process was repeated five times. Subsequently, the temperature was raised gradually until 313 K, reaching a pressure between 85 and 95 bar and affording CO_2 in a supercritical state. Finally, under constant temperature (313K), the chamber was vented at a rate of 8 bar/hour down to atmospheric pressure.

pH measurements were carried out with a Mettler-Toledo LE422 electrode connected to a DrDAQ data logger from Pico Techonology equipped with a DD100 temperature sensor.

UV-Visible spectra were recorded in Cary 60 UV-Vis spectrophotometer (Agilent).

Microwave syntheses were performed using an ETHOS 1 Advanced Microwave Digestion Labstation.

Section S2. Synthetic Procedures

Synthesis of TAPB-BTCA-COF. 49 mg of BTCA (0.30 mmol) were dissolved in 110 mL of degassed Milli-Q water. 105 mg of TAPB (0.30 mmol) were dissolved in 110 mL of degassed Milli-Q water and 11 mL of acetic acid. Both solutions were mixed and the reaction mixture was heated at 80 ºC for 5 days under inert atmosphere. The obtained solid was filtered and solvent exchanged four times with ethanol and dried at 150 ºC under vacuum for 24 h. 140.7 mg of a yellow solid were obtained (97 % yield). Elemental analysis of **TAPB-BTCA-COF**: *Calculated for* $C_{33}H_{21}N_3(H_2O)_{1.5}$: C: 81.46 %; H: 4.97 %; N: 8.64 %. *Experimental*: C: 81.92 %; H: 4.90 %; N: 8.70 %.

Synthesis of TZ-BTCA-COF. 32 mg of BTCA (0.20 mmol) were dissolved in 80 mL of degassed Milli-Q water. 70 mg of TZ (0.20 mmol) were dissolved in 0.5 mL of DMSO and then added dropwise to 80 mL of hot degassed Milli-Q water with 8 mL of acetic acid (since TZ is completely planar, the stronger intermolecular stacking interactions make its dissolution kinetics much slower than for TAPB, dissolving it previously in a small amount of DMSO helps to overcome the kinetic barrier for its dissolution). Both solutions were mixed and the reaction mixture was heated at 80 ºC for 5 days under inert atmosphere. The obtained solid was filtered and solvent exchanged four times with hot ethanol and dried under at 150 ºC under vacuum for 24 hours. 91 mg of a yellow solid were obtained (93 % yield). Elemental analysis of **TZ-BTCA-COF**: *Calculated for* $C_{30}H_{18}N_6(H_2O)_{1.5}$: C: 73.61 %; H: 4.32 %; N: 17.17 %. *Experimental*: C: 73.21 %; H: 4.62 %; N: 16.81 %.

Synthesis of HZ-BTCA-COF. 80 mg of BTCA (0.49 mmol) were dissolved in 50 mL of degassed Milli-Q water and 5 mL of acetic acid. 50 µL of hydrazine monohydrate (1.03 mmol) were dissolved in 50 mL of degassed Milli-Q water. Both solutions were mixed and the reaction mixture was heated at 80 ºC for 5 days under inert atmosphere. The obtained solid was filtered and solvent exchanged four times with ethanol and dried by critical point drying. 72 mg of a yellow solid were obtained (89 % yield). Elemental analysis of **HZ-BTCA-COF**: *Calculated for* $C_{18}H_{12}N_6(H_2O)$: C: 65.44 %; H: 4.27 %; N: 25.44 %. *Experimental*: C: 65.56 %; H: 4.30 %; N: 23.15 %.

Synthesis of RT TAPB-BTCA-COF. 23 mg of BTCA (0.14 mmol) were dissolved in 58 mL of degassed Milli-Q water. 50 mg of TAPB (0.14 mmol) were dissolved in 58 mL of degassed Milli-Q water and 5.8 mL of acetic acid. Both solutions were mixed and the reaction mixture was heated at 35 ºC for 5 days under inert atmosphere. The obtained solid was filtered and solvent exchanged four times with ethanol and dried at 150 ºC under vacuum for 24 hours. 61.2 mg of a yellow solid were obtained (90 % yield).

Synthesis of MW TAPB-BTCA-COF. 12 mg of BTCA (0.075 mmol) were dissolved in 37.5mL of degassed Milli-Q water. 26 mg of TAPB (0.075 mmol) were dissolved in 37.5 mL of degassed Milli-Q water and 3.75 mL of acetic acid. Both solutions were transferred to a (75 mL x5) microwave glass vessel and heated at 80 ºC for 300 min. The solid obtained was filtered and solvent exchanged four times with ethanol and dried at 150 ºC under vacuum for 24 h. 30.7 mg of a yellow solid were obtained (85 % yield).

Section S3. Characterization of TAPB-BTCA-COF

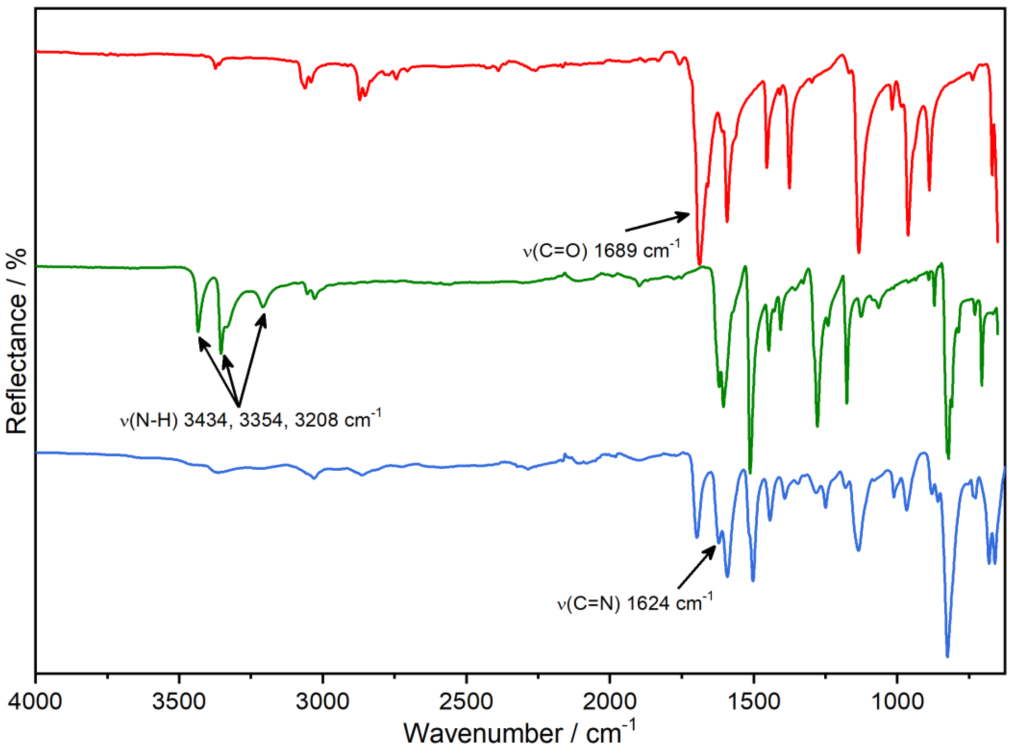

Figure S1. ATR-FT-IR spectra of **BTCA** (red), **TAPB** (green), and **TAPB-BTCA-COF** (blue).

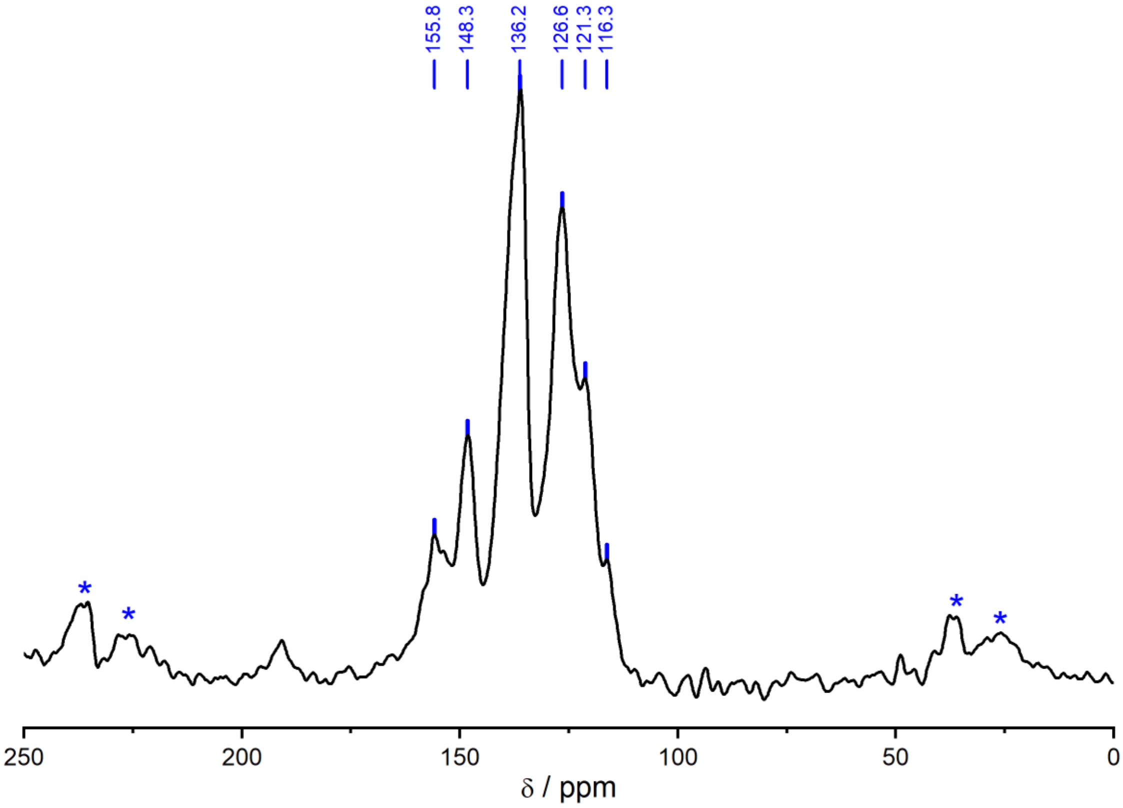

Figure S2. ^{13}C CP-MAS solid-state NMR of **TAPB-BTCA-COF**. Asterisks denote spinning side bands.

Table S1. Molecular model of **TAPB-BTCA-COF** and ^{13}C NMR spectrum peak assignment.

	Assignment	Signal (ppm)
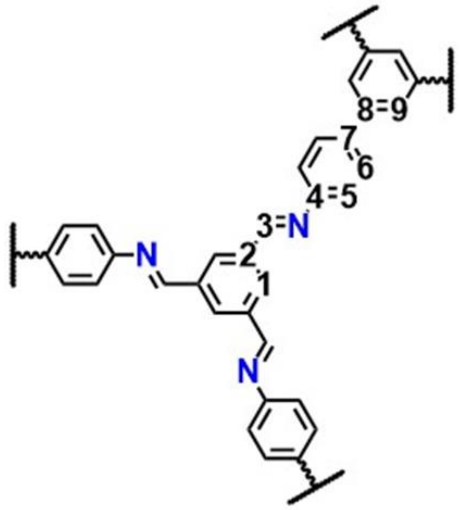	1,2	137.1
	3	155.8
	4	148.3
	5	116.3
	6,7	126.6
	8	137.1
	9	121.3

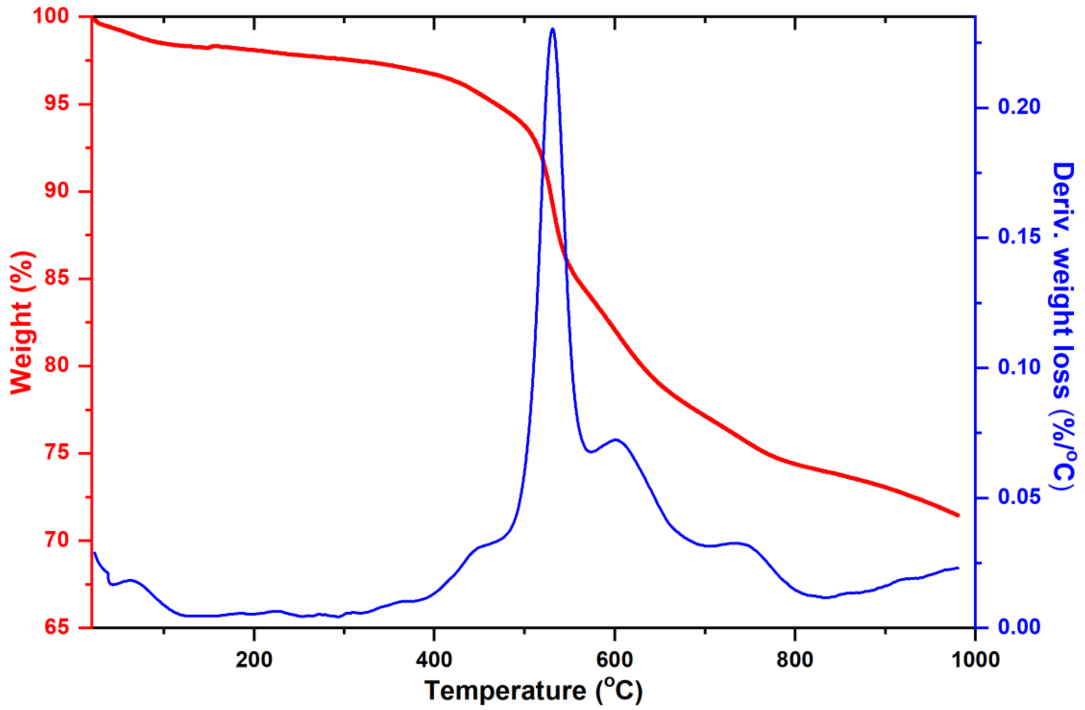

Figure S3. TGA trace (red) and derivative of weight loss (blue) of **TAPB-BTCA-COF**.

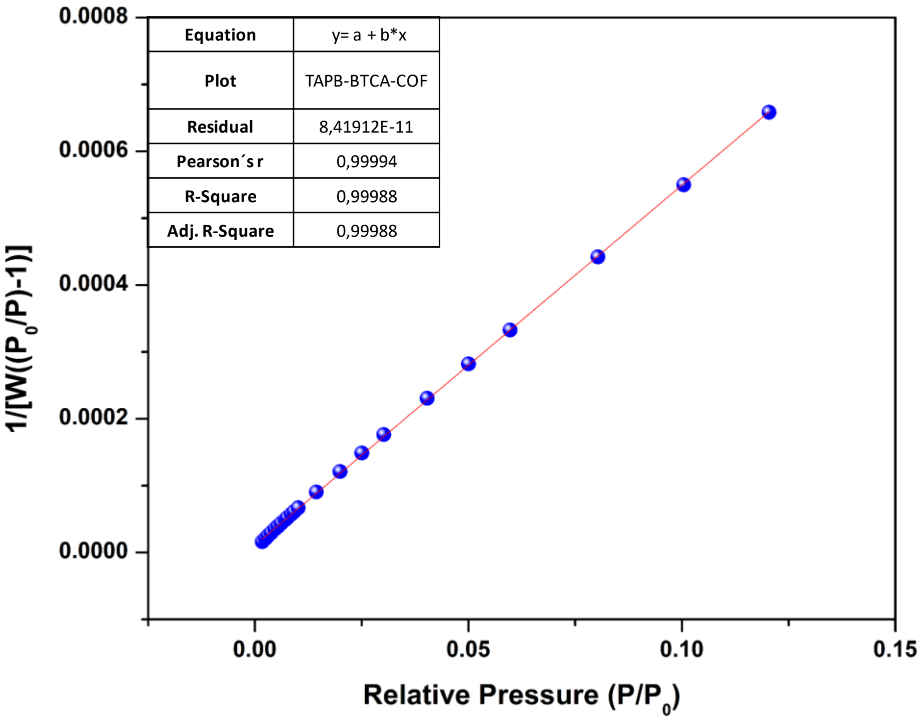

Equation	y= a + b*x
Plot	TAPB-BTCA-COF
Residual	8,41912E-11
Pearson´s r	0,99994
R-Square	0,99988
Adj. R-Square	0,99988

Figure S4. BET plot for N_2 sorption in **TAPB-BTCA-COF**.

Table S2. BET surface area (SA_{BET}) values of **TAPB-BTCA-COF**.

Solvent	**Temperature (ºC)**	**Time (h)**	**Surface area (m^2 g^{-1})**	**Ref.**
m-cresol	Room temperature	72	329	1
Acetic acid	Room temperature	72	700	4
Dioxane with 6 M aqueous acetic acid	120	72	435	5
Dioxane:mesitylene 5:1 with 10 M aqueous acetic acid	80	168	1120	6
Dioxane:mesitylene 1:1 with 6 M aqueous acetic acid	120	168	1268	7
THF:mesitylene 3:1 with 6 M aqueous acetic acid	120	72	922	8
Dioxane:mesitylene 5:1 with 25 M acetic acid	100	168	684	9
Dioxane:mesitylene 1:9 with 6 M aqueous acetic acid	120	72	409	9
Water	80	120	806	This work
Water	Room temperature	120	803	This work
Water	80 (microwave irradiation)	5	566	This work

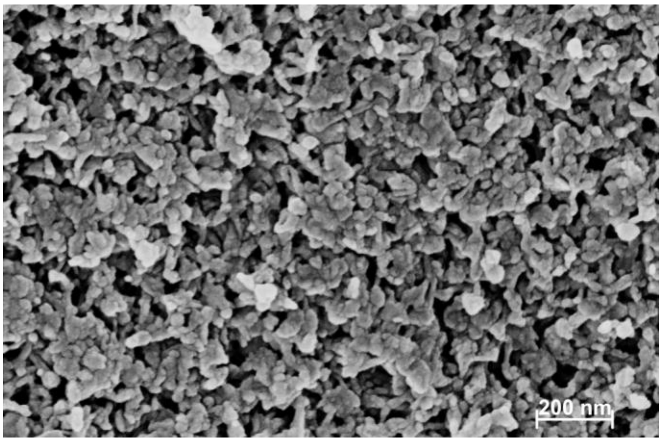

Figure S5. Representative SEM image of **TAPB-BTCA-COF** showing the assembly of nanocrystals.

Section S4. Effect of the pH on TAPB-BTCA-COF synthesis

Experimental procedure: 5.3 mg of BTCA were dissolved in 14 mL of Milli-Q water. 11.5 mg of TAPB were dissolved (or suspended if not completely soluble) in 14 mL of aqueous acetic acid solutions of different concentrations. The concentration of acetic acid was adjusted to obtain the desired pH value (which was confirmed and finely tuned using a pH meter). The BTCA and TAPB solutions were mixed, and subsequently, the pH was measured. Then, the reaction mixture was heated at 80 °C for 5 days under inert atmosphere. Finally, the solid was filtered, washed with ethanol and dried in vacuum at 150 °C for 24 h in order to record the yield.

Table S3. Yields of **TAPB-BTCA-COF** synthesized at different pH values.

pH	Yield (%)
2.0	0
2.4	90
3.0	33
3.5	10
4.0	1

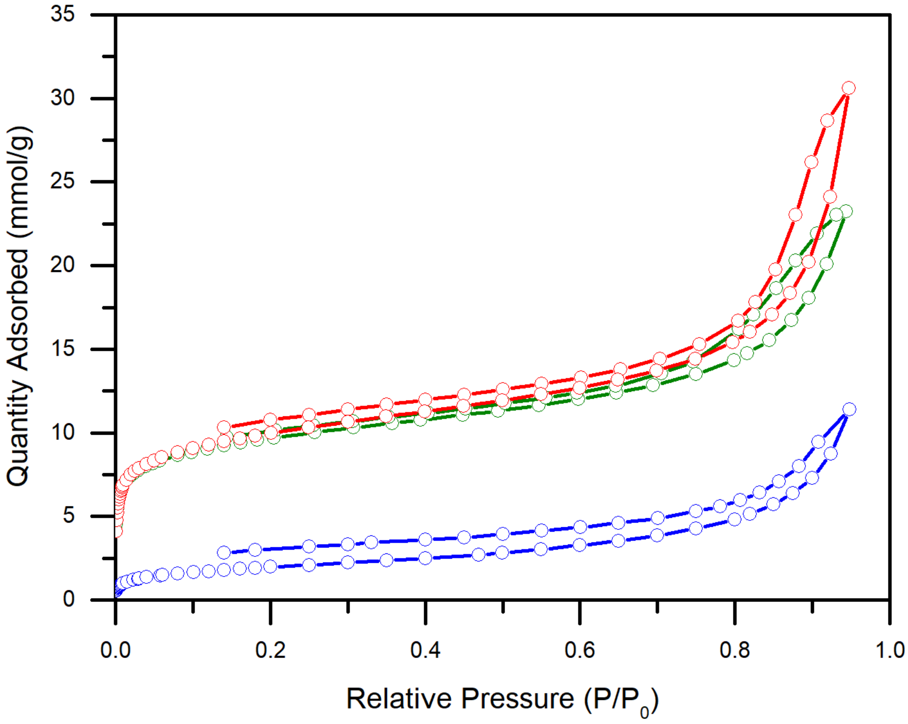

Figure S6. N_2 adsorption–desorption isotherm of **TAPB-BTCA-COF** synthesized at pH values of 2.4 (red), 3 (green) and 3.5 (blue).

Table S4. BET surface area (SA_{BET}) values of **TAPB-BTCA-COF** synthesized at different pH values.

pH	**2.4**	**3.0**	**3.5**
Surface area ($m^2\ g^{-1}$)	806	780	150

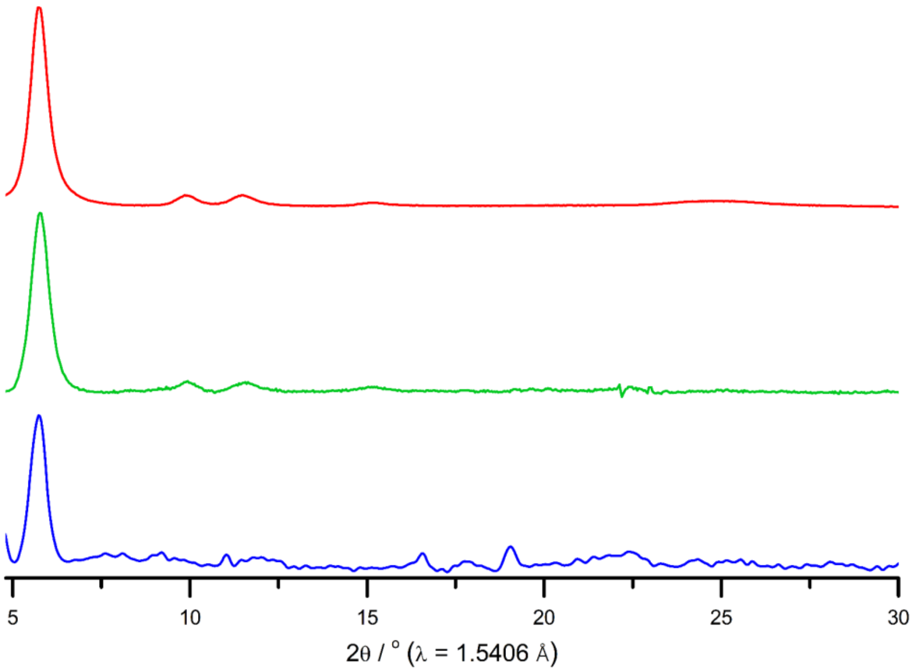

Figure S7. PXRD patterns of **TAPB-BTCA-COF** synthesized at pH values of 2.4 (red), 3 (green) and 3.5 (blue).

Solubility measurements: The UV-Visible spectra of **TAPB** solutions with concentrations between 0.005 and 0.1 mM in water at pH 2.4 (adjusted with acetic acid) were recorded to obtain a calibration curve at λ = 280 nm (R^2 = 0.9998).

Aqueous solutions of acetic acid at pH 2.4, 3.0, 3.5 and 4.0 were saturated with **TAPB**, ultrasonicated and kept at 35 ºC for 24 h, to ensure that equilibrium was reached. The solutions were centrifuged for 2 min at 5000 rcf, the supernatant was isolated and diluted with an aqueous solution of acetic acid at pH 2.4. The UV-Visible spectra of these solutions were recorded and the concentration calculated using the calibration curve.

Table S5. Solubility of TAPB at different pH values.

pH	**2.4**	**3.0**	**3.5**	**4.0**
TAPB solubility (mM)	5.065	0.216	0.109	0.031

pK_a measurement: 32 mg of **TAPB** were dissolved in 3 mL of THF and acidified with 50 µL of concentrated HCl. The white precipitate was washed with 5 mL of THF and 5 mL of ethanol. Finally, it was dried in vacuum to obtain 31 mg of TAPB trihydrochloride (**(H_3TAPB)Cl_3**).

(H_3TAPB)Cl_3 was dissolved in Milli-Q water at concentrations ranging between 0.002 and 0.04 M, and the pH of those solutions was measured. The pH *vs* **TAPB** concentration data was plotted and fitted to Equation 1.

$pH = -log\frac{-K_a+\sqrt{{K_a}^2+4\,K_a\,C}}{2}$ Equation 1. K_a is the acid dissociation constant of **(H_3TAPB)Cl_3** and C is the concentration of **TAPB**.

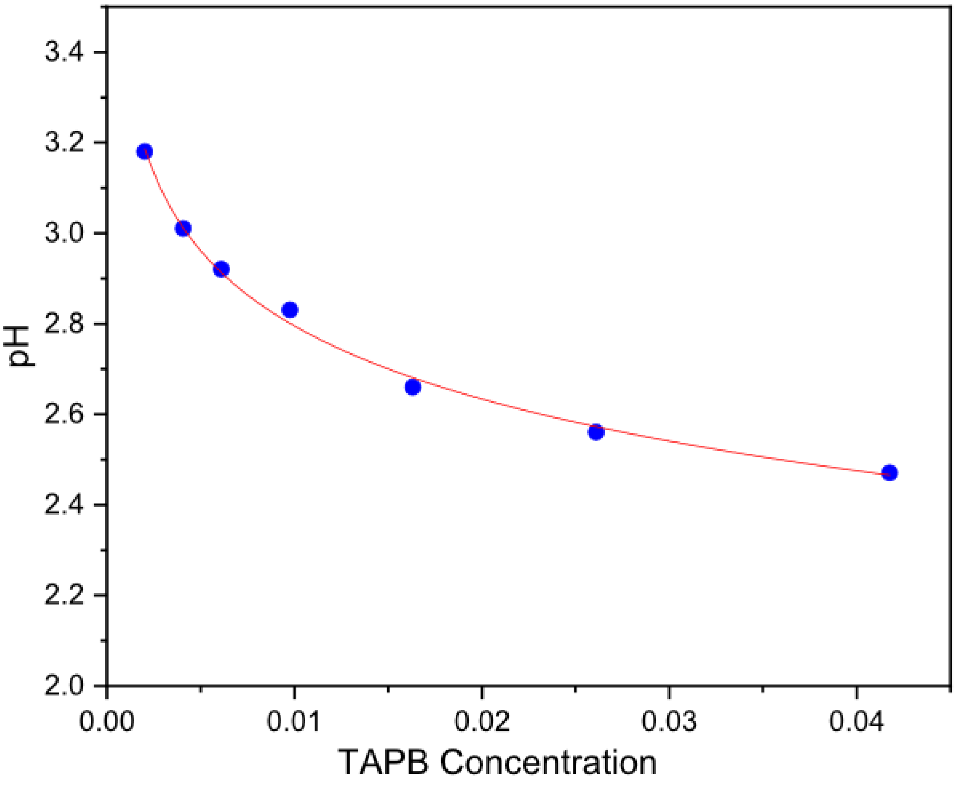

Figure S8. pH of **(H_3TAPB)Cl_3** solutions of different concentration (blue dots) and non-linear fit of the data to Equation 1 (red line), with Ka = 3.5.

Section S5. Effect of concentration on TAPB-BTCA-COF synthesis

Synthesis of TAPB-BTCA-COF. 49 mg of BTCA (0.30 mmol) were dissolved in 55 mL of degassed Milli-Q water. 105 mg of TAPB (0.30 mmol) were dissolved in 55 mL of degassed Milli-Q water and 5.5 mL of acetic acid. Both solutions were mixed and the reaction mixture was heated at 80 ºC for 5 days under inert atmosphere. The obtained solid was filtered and solvent exchanged four times with ethanol and dried at 150 ºC under vacuum for 24 h. 72 mg of a yellow solid were obtained (52 % yield). Elemental analysis of **TAPB-BTCA-COF**: *Calculated for* $C_{33}H_{21}N_3(H_2O)_{1.5}$: C: 81.46 %; H: 4.97 %; N: 8.64 %. *Experimental*: C: 82.14 %; H: 4.99 %; N: 8.60 %.

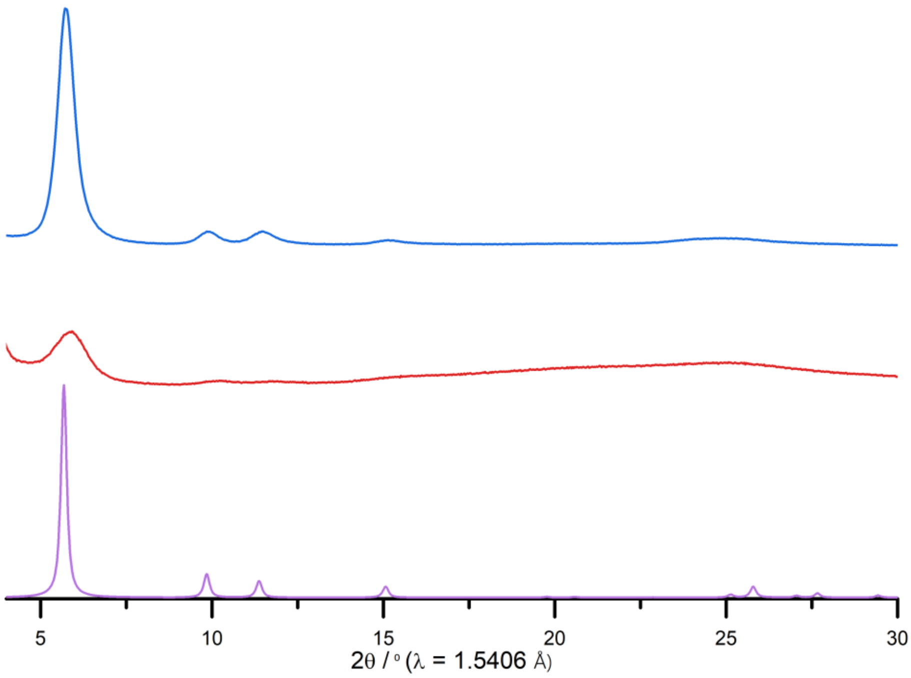

Figure S9. PXRD patterns of **TAPB-BTCA-COF** (blue), **TAPB-BTCA-COF** synthesized with double concentration of monomers (red) and simulated (purple).

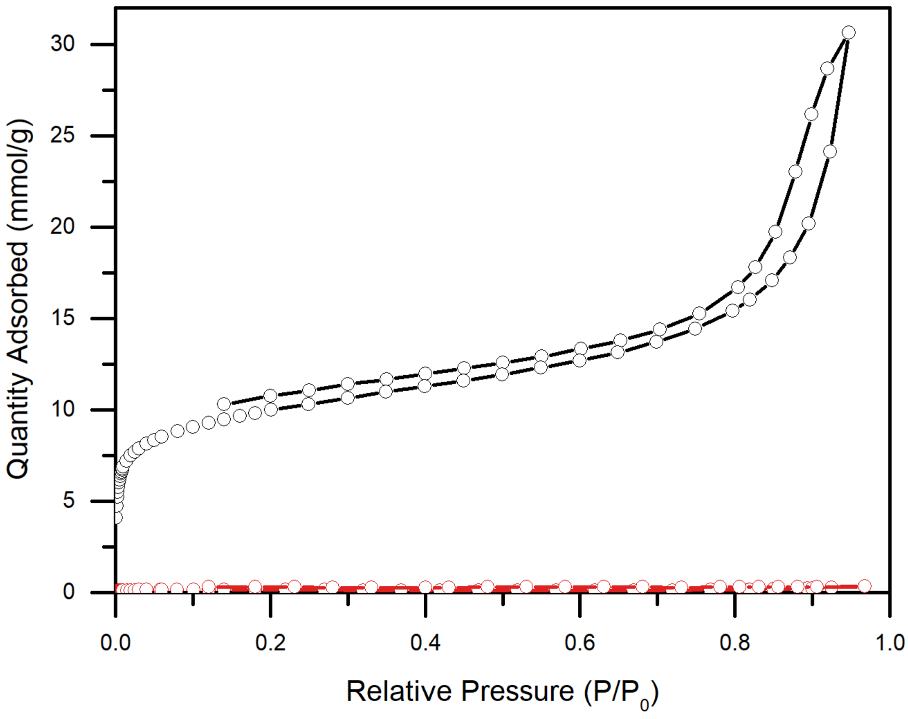

Figure S10. N_2 adsorption–desorption isotherm of **TAPB-BTCA-COF** (black) and **TAPB-BTCA-COF** synthesized with double concentration of monomers (red).

Section S6. Characterization of HZ-BTCA-COF and TZ-BTCA-COF

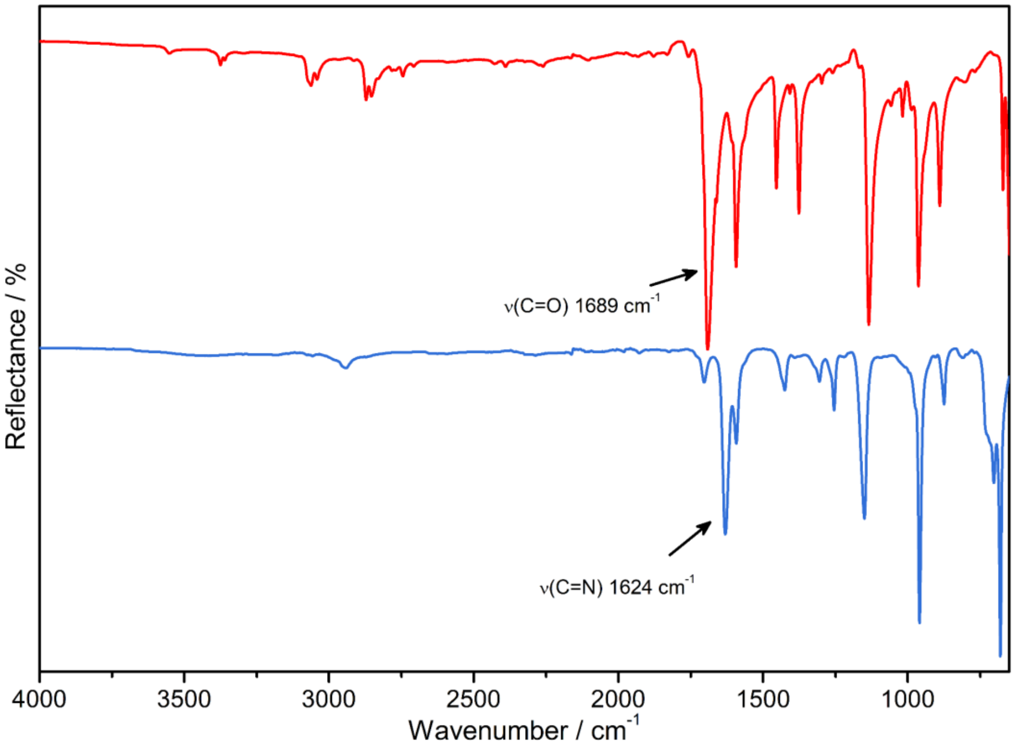

Figure S11. ATR-FT-IR spectra of **BTCA** (red) and **HZ-BTCA-COF** (blue).

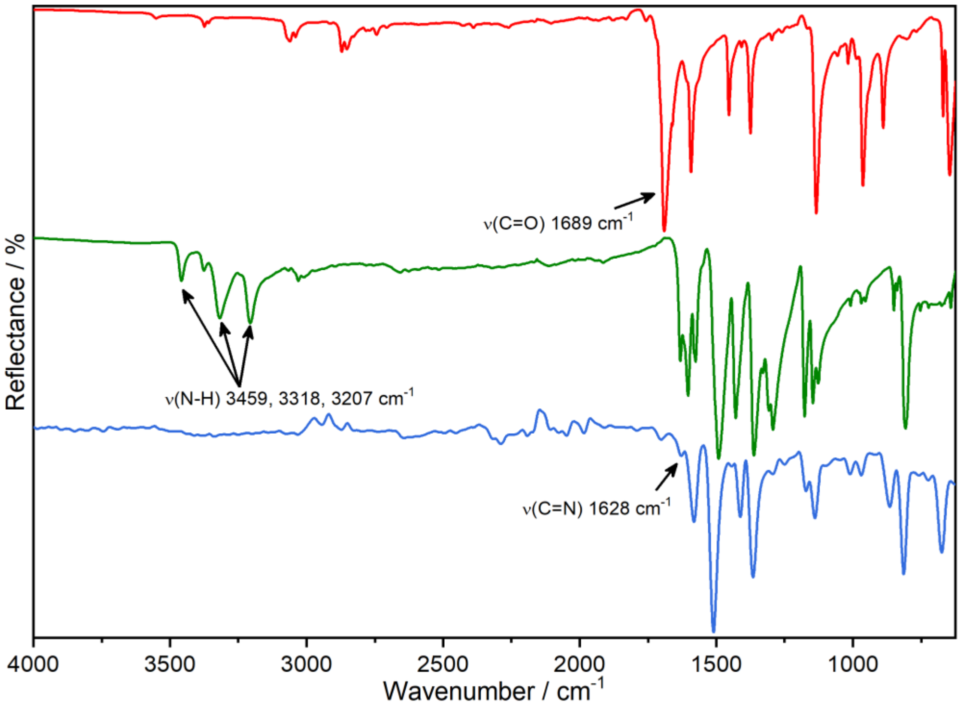

Figure S12. ATR-FT-IR spectra of **BTCA** (red), **TZ** (green), and **TZ-BTCA-COF** (blue).

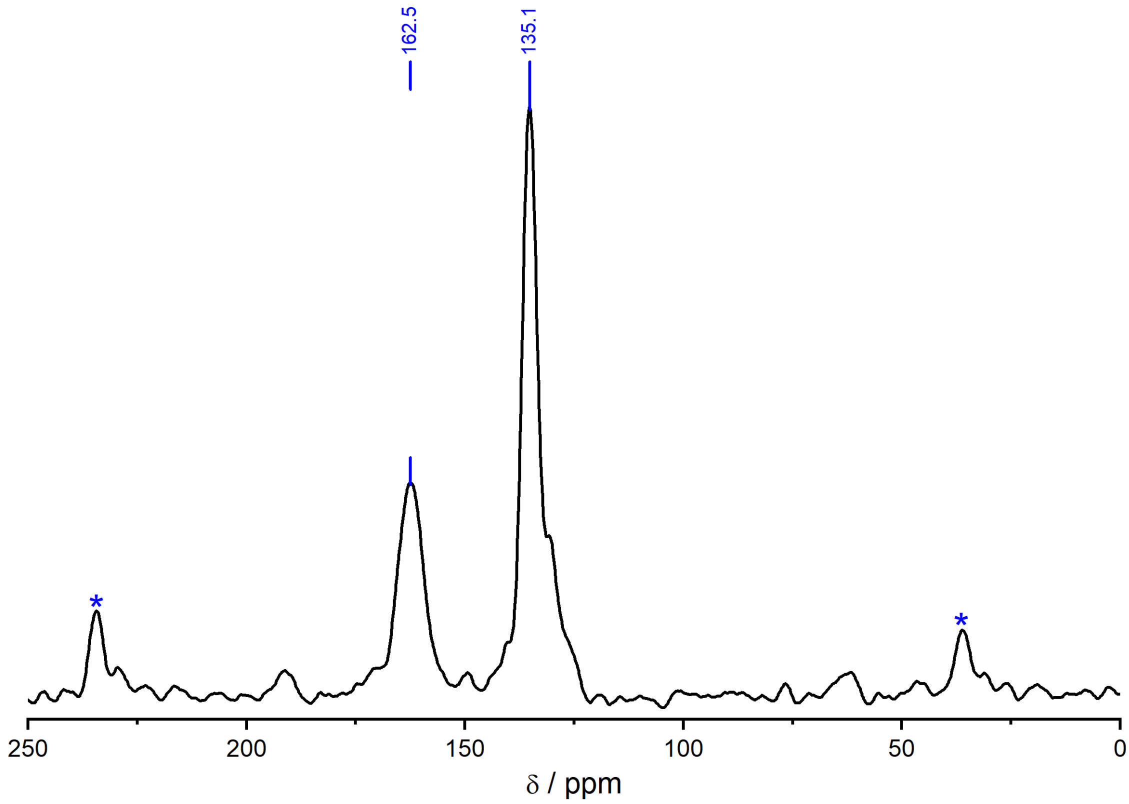

Figure S13. ^{13}C CP-MAS solid-state NMR of **HZ-BTCA-COF**. Asterisks denote spinning side bands.

Table S6. Molecular model of **HZ-BTCA-COF** and ^{13}C NMR spectrum peak assignment.

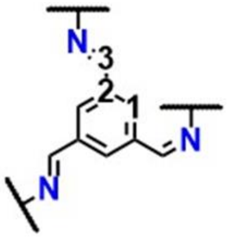	**Assignment**	**Signal (ppm)**
	1	135.1
	2	135.1
	3	162.3

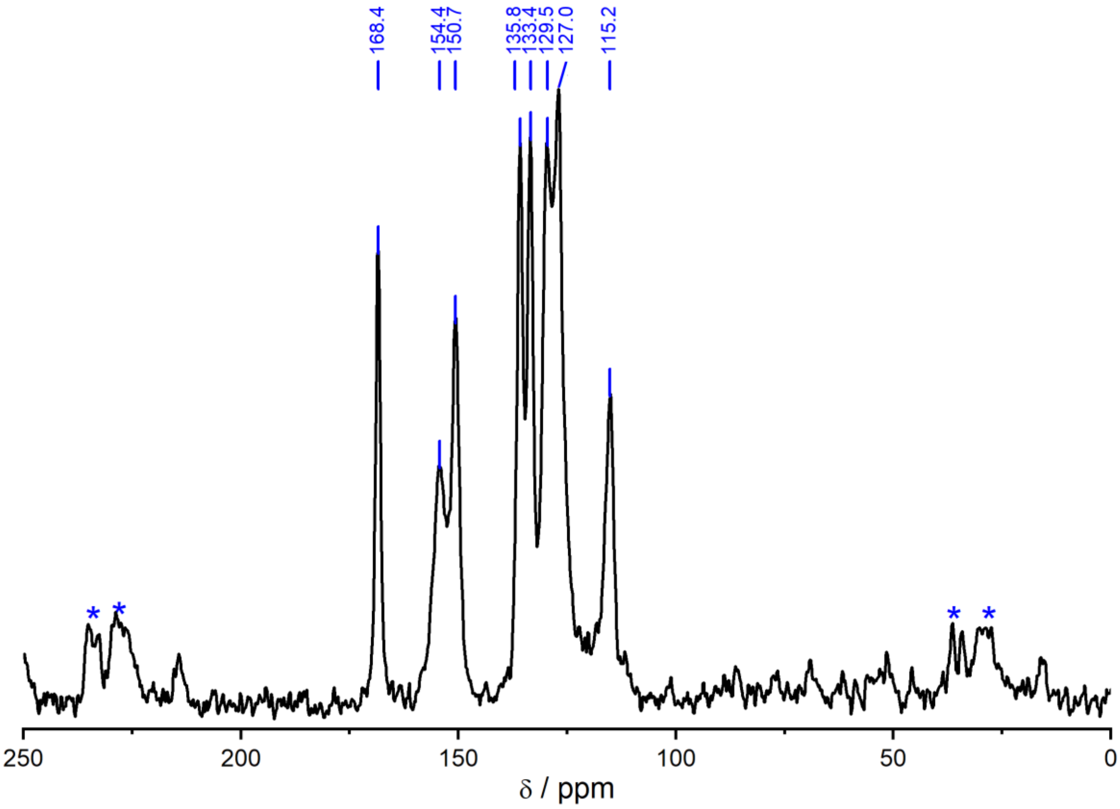

Figure S14. ^{13}C CP-MAS solid-state NMR of **TZ-BTCA-COF**. Asterisks denote spinning side bands.

Table S7. Molecular model of **TZ-BTCA-COF** and ^{13}C NMR spectrum peak assignment.

	Assignment	**Signal (ppm)**
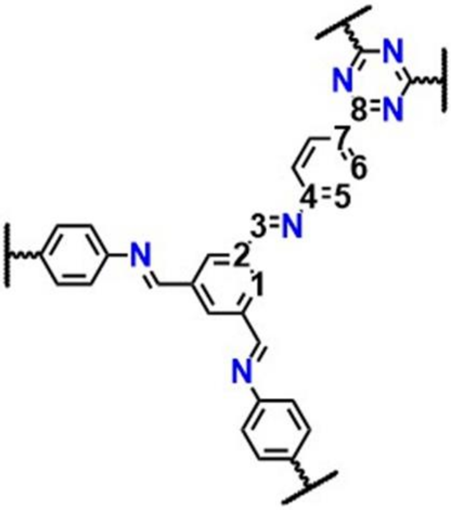	1	135.8
	2	133.4
	3	154.4
	4	150.7
	5	115.2
	6	127.1
	7	129.7
	8	168.5

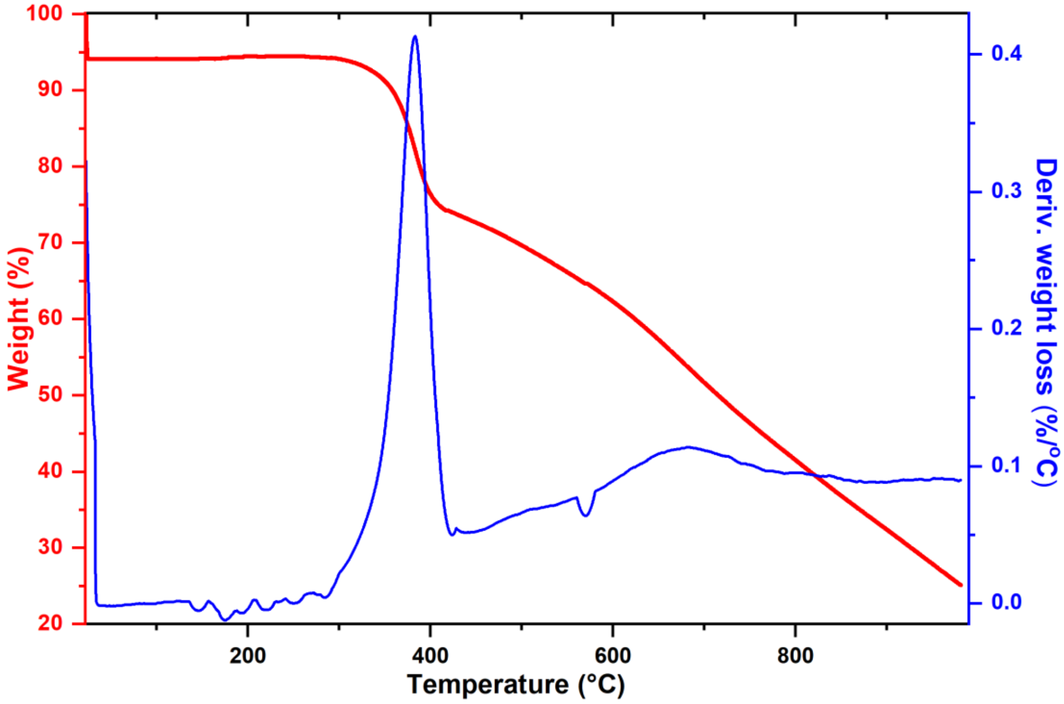

Figure S15. TGA trace (red) and derivative of weight loss (blue) of **HZ-BTCA-COF**.

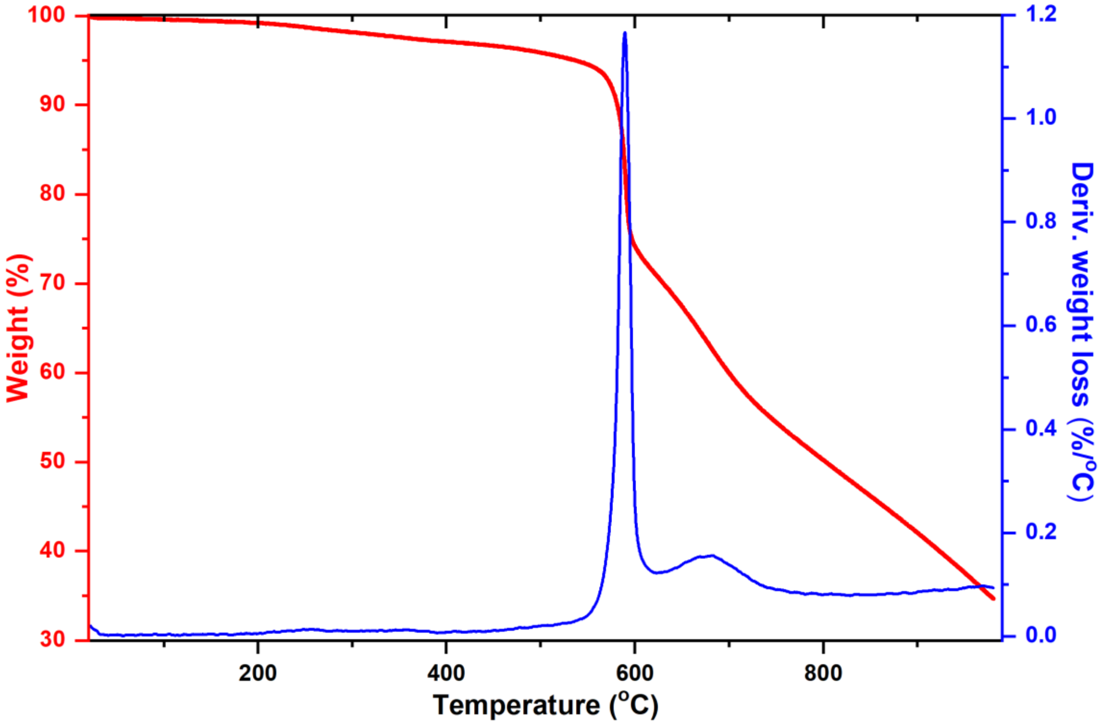

Figure S16. TGA trace (red) and derivative of weight loss (blue) of **TZ-BTCA-COF**.

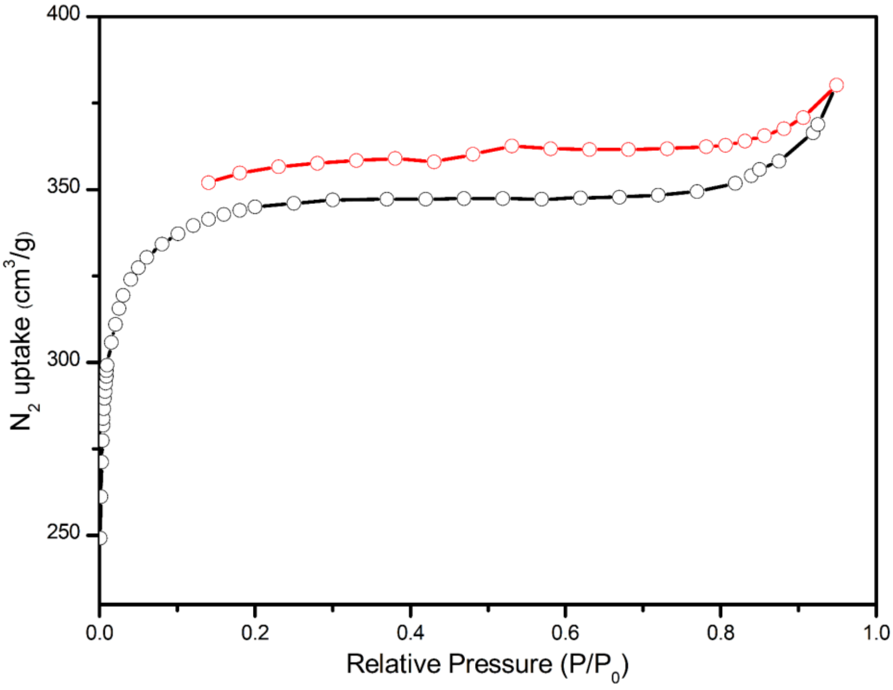

Figure S17. N_2 adsorption–desorption isotherm of **HZ-BTCA-COF.** Adsorption branch in black, desorption branch in red.

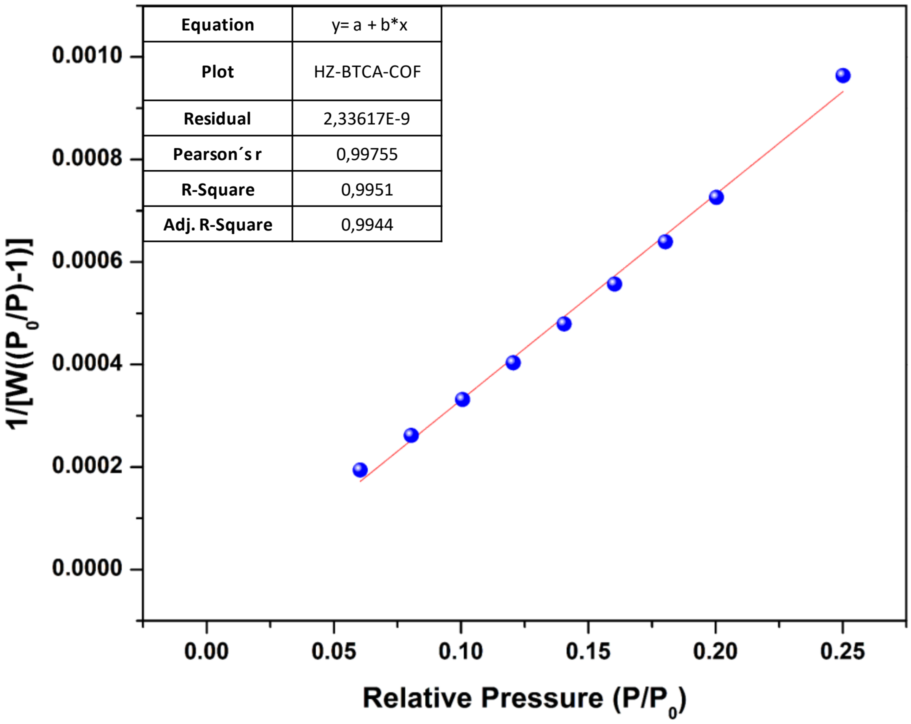

Equation	y= a + b*x
Plot	HZ-BTCA-COF
Residual	2,33617E-9
Pearson´s r	0,99755
R-Square	0,9951
Adj. R-Square	0,9944

Figure S18. BET plot for N_2 sorption in **HZ-BTCA-COF**.

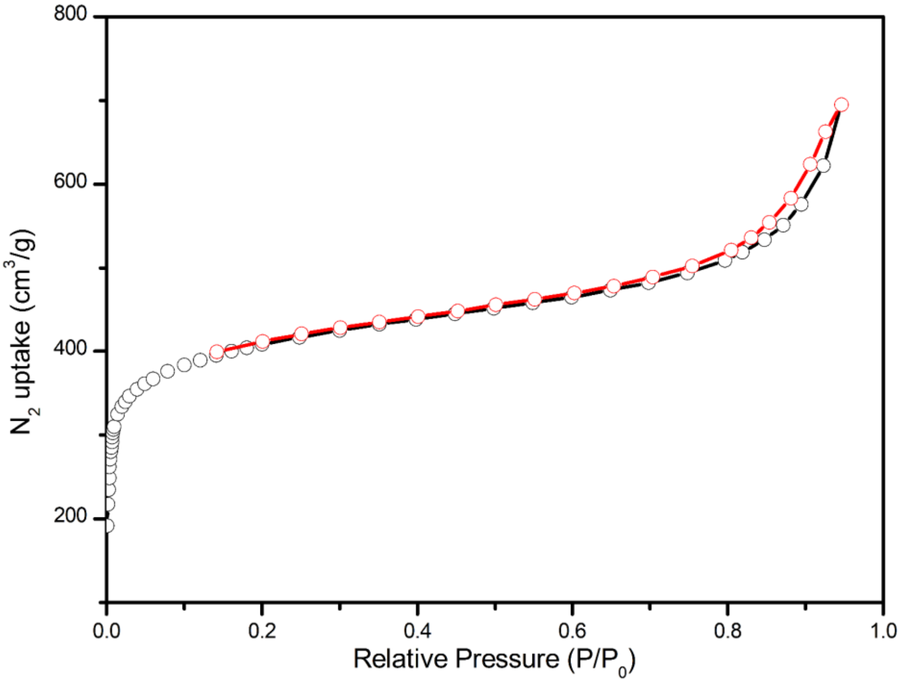

Figure S19. N_2 adsorption–desorption isotherm of **TZ-BTCA-COF.** Adsorption branch in black, desorption branch in red.

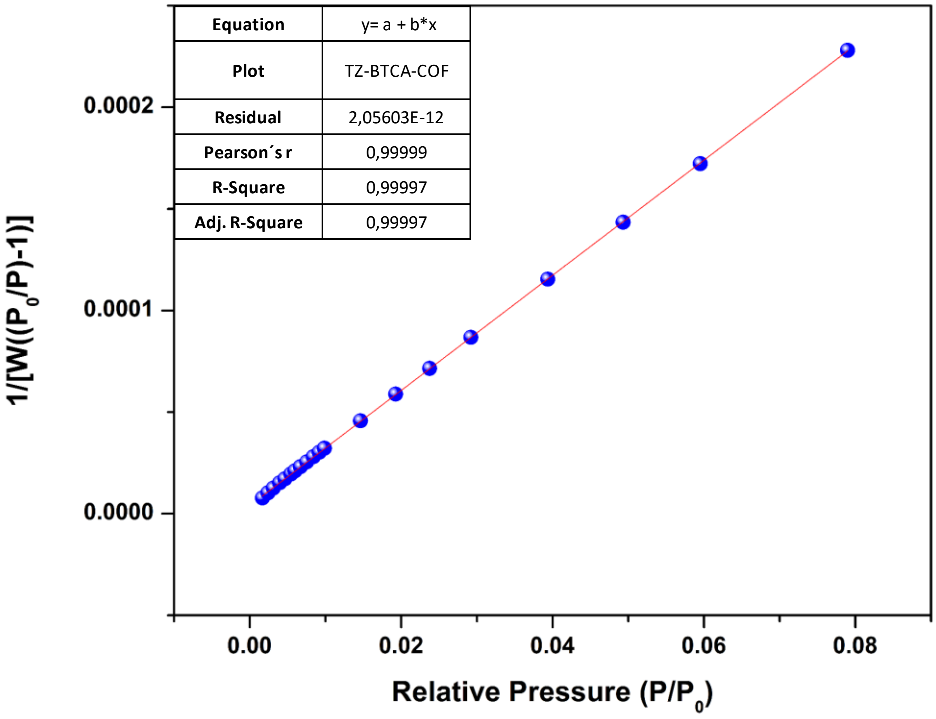

Equation	y= a + b*x
Plot	TZ-BTCA-COF
Residual	2,05603E-12
Pearson´s r	0,99999
R-Square	0,99997
Adj. R-Square	0,99997

Figure S20. BET plot for N_2 sorption in **TZ-BTCA-COF**.

Section S7 Characterization of RT TAPB-BTCA-COF

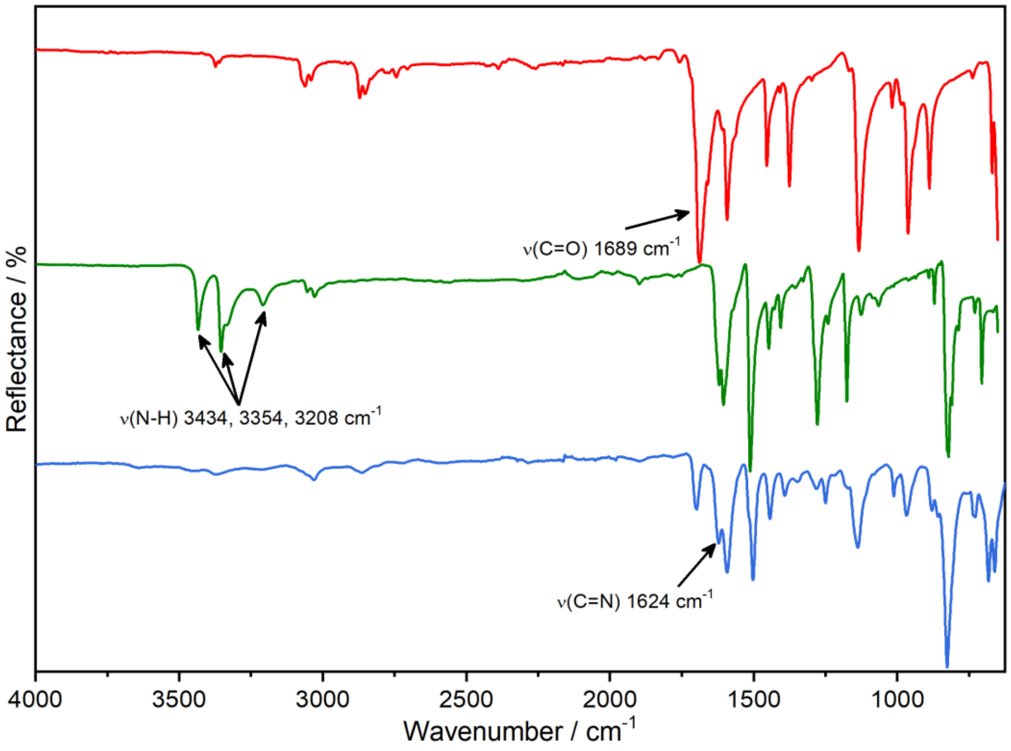

Figure S21. ATR-FT-IR spectra of **BTCA** (red), **TAPB** (green), and **RT TAPB-BTCA-COF** (blue).

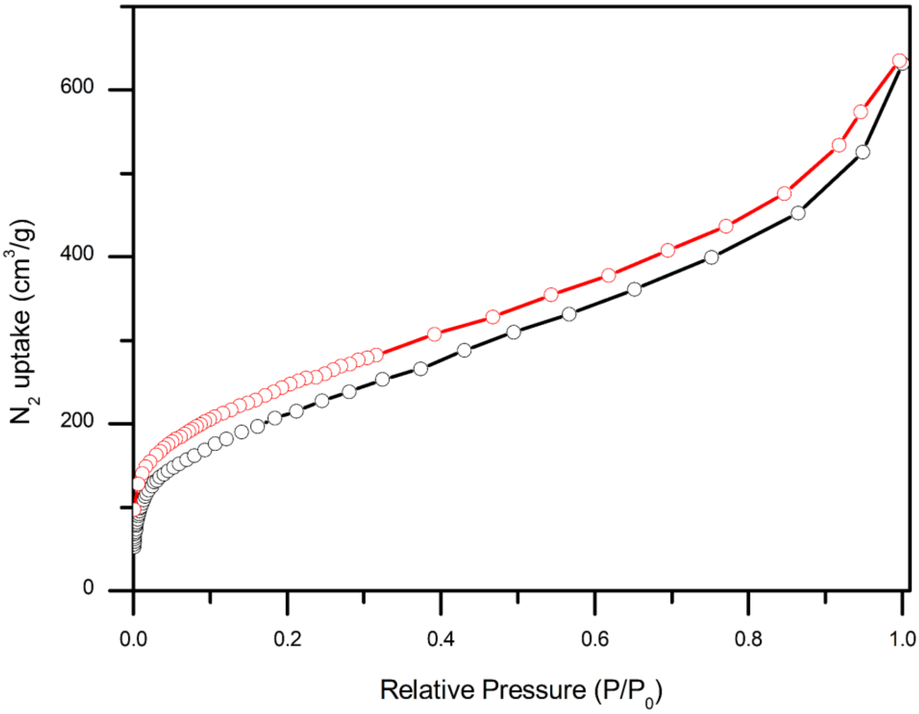

Figure S22. N_2 adsorption–desorption isotherm of **RT TAPB-BTCA-COF.** Adsorption branch in black, desorption branch in red.

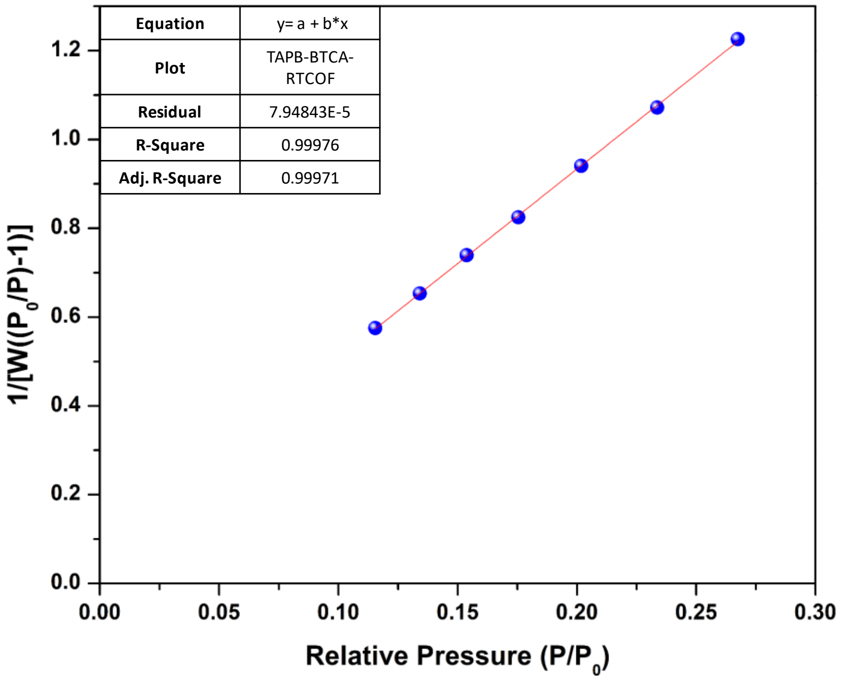

Figure S23. BET plot for N_2 sorption in **RT TAPB-BTCA-COF**.

Section S8 Characterization of MW TAPB-BTCA-COF

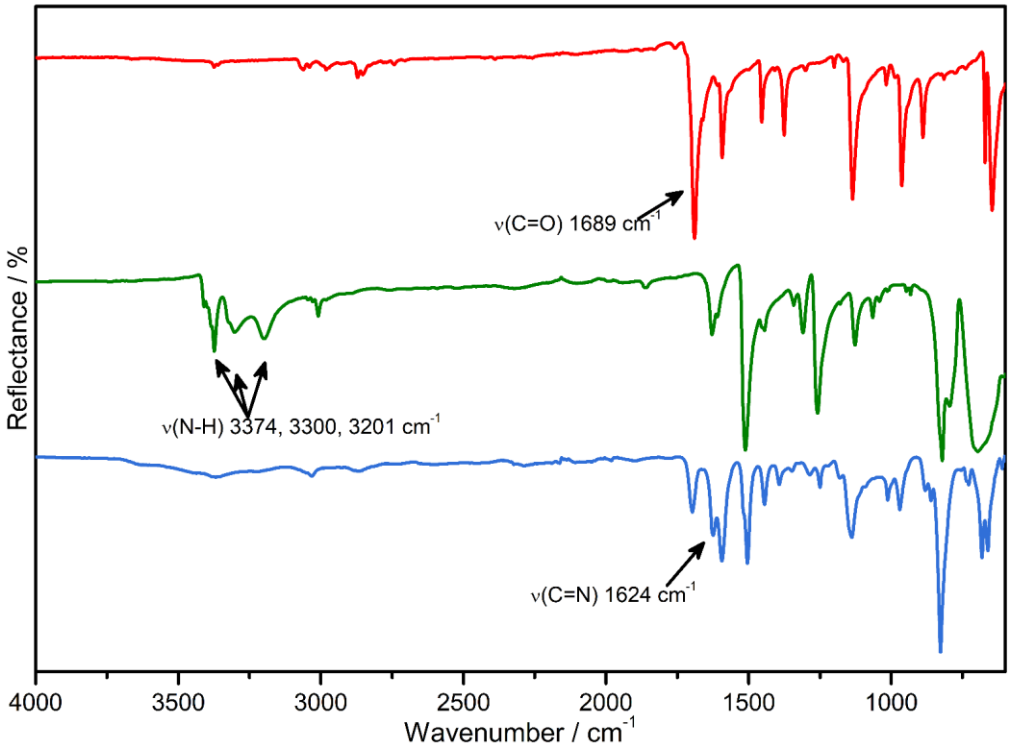

Figure S24. ATR-FT-IR spectra of **BTCA** (red), **TAPB** (green), and **MW TAPB-BTCA-COF** (blue).

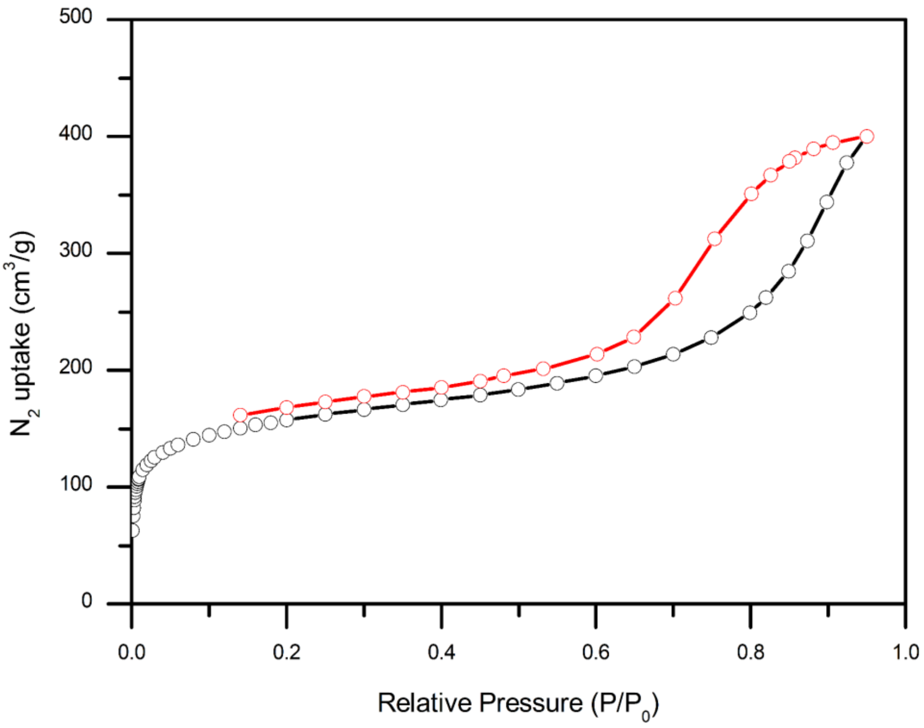

Figure S25. N_2 adsorption–desorption isotherm of **MW TAPB-BTCA-COF.** Adsorption branch in black, desorption branch in red.

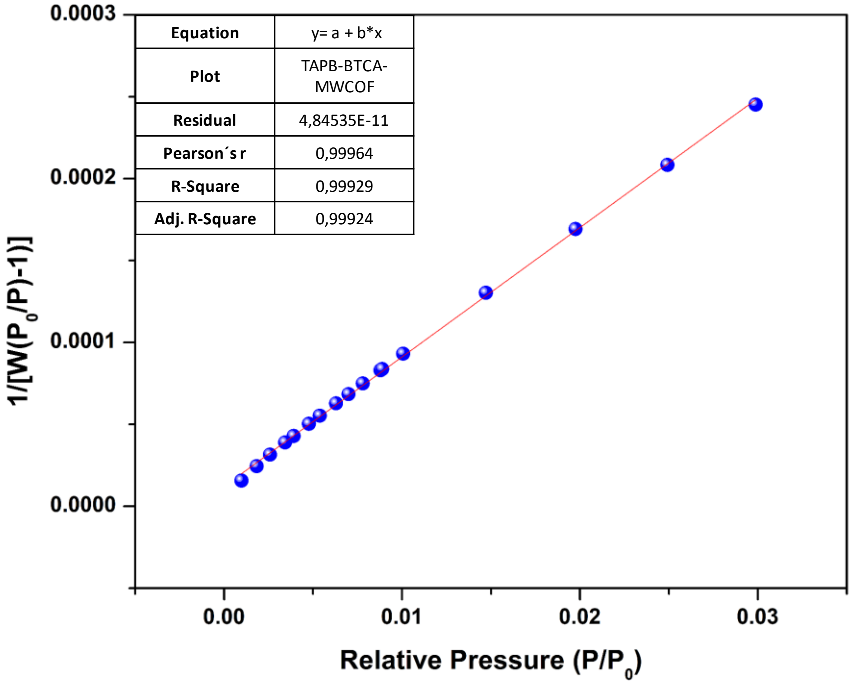

Figure S26. BET plot for N_2 sorption in **MW TAPB-BTCA-MCOF**.

Section S9 Simulation of the accessible surface area

Table S8. Accessible surface areas calculated using different software

	Surface areas*(m^2 g^{-1})	**Surface area** (m^2 g^{-1})**
TAPB-BTCA-COF	1499	1829
HZ-BTCA-COF	1454	1989
TZ-BTCA-COF	1502	1955

*Poreblazer software ** Material Studio software (Connolly surface)

Section S10 References

[1] A. de la Peña Ruigómez, D. Rodríguez-San-Miguel, K. C. Stylianou, M. Cavallini, D. Gentili, F. Liscio, S. Milita, O. M. Roscioni, M. L. Ruiz-González, C. Carbonell, D. Maspoch, R. Mas-Ballesté, J. L. Segura and F. Zamora, *Chemistry - A European Journal*, 2015, **21**, 10666–10670.

[2]L. Sarkisov and A. Harrison, *Mol. Simul*., 2011, **37**, 1248-1257.

[3]J. Lee, J. H. Kwak and W. Choe*, Nat Commun*, 2017, **8**, 14070.

[4]D. Rodríguez-San-Miguel, A. Abrishamkar, J. A. R. Navarro, R. Rodriguez-Trujillo, D. B. Amabilino, R. Mas-Ballesté, F. Zamora and J. Puigmartí-Luis, *Chem. Commun.*, 2016, **52**, 9212–9215.

[5]J. Dong, Y. Wang, G. Liu, Y. Cheng and D. Zhao, *CrystEngComm*, 2017, **19**, 4899–4904.

[6]D. Rodríguez-San-Miguel, A. Yazdi, V. Guillerm, J. Pérez-Carvajal, V. Puntes, D. Maspoch and F. Zamora, *Chem. Eur. J.*, 2017, **23**, 8623–8627.

[7]X. Li, Q. Gao, J. Aneesh, H.-S. Xu, Z. Chen, W. Tang, C. Liu, X. Shi, K. V. Adarsh, Y. Lu and K. P. Loh, *Chem. Mater.*, 2018, **30**, 5743–5749.

[8]M. C. Daugherty, E. Vitaku, R. L. Li, A. M. Evans, A. D. Chavez and W. R. Dichtel, *Chem. Commun.*, 2019, **55**, 2680–2683.

[9]A. Jiménez-Almarza, A. López-Magano, L. Marzo, S. Cabrera, R. Mas-Ballesté and J. Alemán, *ChemCatChem*, 2019, **11**, 4916–4922.